

University of Warwick institutional repository: <http://go.warwick.ac.uk/wrap>

This paper is made available online in accordance with publisher policies. Please scroll down to view the document itself. Please refer to the repository record for this item and our policy information available from the repository home page for further information.

To see the final version of this paper please visit the publisher's website. Access to the published version may require a subscription.

Author(s): S. Dixon, M. P. Fletcher, and G. Rowlands

Article Title: The accuracy of acoustic birefringence shear wave measurements in sheet metal

Year of publication: 2008

Link to published article:

<http://dx.doi.org/10.1063/1.3033395>

Publisher statement: Copyright (2008) American Institute of Physics. This article may be downloaded for personal use only. Any other use requires prior permission of the author and the American Institute of Physics.

Citation: Dixon, S. et al. (2008). The accuracy of acoustic birefringence shear wave measurements in sheet metal. *Applied Physics Letters*, Vol. 104, No. 11, 114901

The accuracy of acoustic birefringence shear wave measurements in sheet metal

S.Dixon^{a)}, M.P. Fletcher and G. Rowlands

Department of Physics, University of Warwick, CV4 7AL, England

Abstract. In rolled metal sheet the through thickness shear wave energy is steered into two orthogonal polarizations, parallel and perpendicular to the sheet's rolling direction. Ultrasonic velocity measurements used to determine the orientation distribution coefficients in thin sheets can be obtained from the fast Fourier transform of the time domain signal. It is observed that the data obtained using a linearly polarized electromagnetic acoustic transducer (EMAT) does not correspond with that obtained using a radially polarized EMAT. An analytical model has been developed which explains the source of this effect from the using the fast Fourier transform.

I. INTRODUCTION

The anisotropy or crystallographic texture [1, 2] of rolled metal sheet gives rise to an effect known as acoustic birefringence [3, 4], whereby the energy of a through thickness shear wave (SH) can be guided into two orthogonal polarizations. Each polarization has a slightly different ultrasonic velocity, approximately parallel and perpendicular to the rolling direction and is termed birefringence. In a magnitude fast Fourier Transform (FFT) [5], birefringence can be seen as two closely spaced peaks (FIG. 1). These peaks occur at multiple frequencies corresponding to an integer number of half-wavelength, ultrasonic, through thickness resonances of the test sample. FFTs are used primarily because they provide a solution where temporal interference would otherwise make it inherently difficult to extract information about closely spaced frequencies in the time domain. Birefringence can be used to at least partially characterise the texture of

metals [6], or the state of their plane stresses [7, 8]. For an aggregate of cubic crystallites, as for the aluminium samples described here, the orientation distribution coefficients (ODCs) that quantify the texture and can be obtained from shear wave measurements are W_{400} and W_{420} [9]. Subsequently these ODCs can be used to predict the behaviour of the material during the cold forming stages of product manufacture, particularly where there is extra empirical data that would help to correlate the shear wave elastic properties to the plastic properties, for the particular alloy concerned.

Acoustic birefringence can be measured using a radially polarized electromagnetic acoustic transducer (EMAT) [10, 11] allowing both polarizations of the shear wave to be captured in the time domain, at the same time. Alternatively, one could use a linearly polarized shear wave transducer, either piezoelectric or an EMAT, polarized at 45° to the rolling direction to capture the two polarizations simultaneously. In all the experiments described here, a wideband pulse-echo [12] EMAT system was used so that all harmonic peaks corresponding to the resonant through thickness shear modes of the sheet could be observed simultaneously, and the same position on the sample for all measurements. The only modification to the captured time domain data was the addition of 2×10^5 zero padding points. Applying a Hanning function in the time domain would also affect the peak positions when more than single frequency is present in the time domain waveform, and has not been done here.

To capture the ultrasonic waveforms for shear waves polarized at 0° and 90° to the rolling direction, one should perform each measurement separately. If the time domain data from a radially polarized EMAT is used to calculate the magnitude FFT, it yields the solid line shown in FIG. 1. A linearly polarized EMAT orientated at 45° to the rolling direction yields a similar magnitude FFT to the radially polarized EMAT. Using a linearly polarized EMAT orientated at 0° and 90° to the rolling direction of the sample yields the magnitude FFTs shown as the dashed line and cross symbols respectively, after processing the time domain data. FIG. 1 also shows that the positions of the magnitude FFT peak maxima do not coincide when comparing data from a radially and linearly polarized EMATs orientated at 0° and 90° to the rolling direction.

^{a)} Electronic mail: s.m.dixon@warwick.ac.uk

The use of contact shear wave probes on the sample at angles of 0° , 45° and 90° , yields similar results to those shown in figure 1. EMATs are however favoured when circumstances require accurate reproducibility, given the inherent variability in thickness of the coupling layer when using piezoelectric transducers and how this can affect the resonant modes of the sample [13].

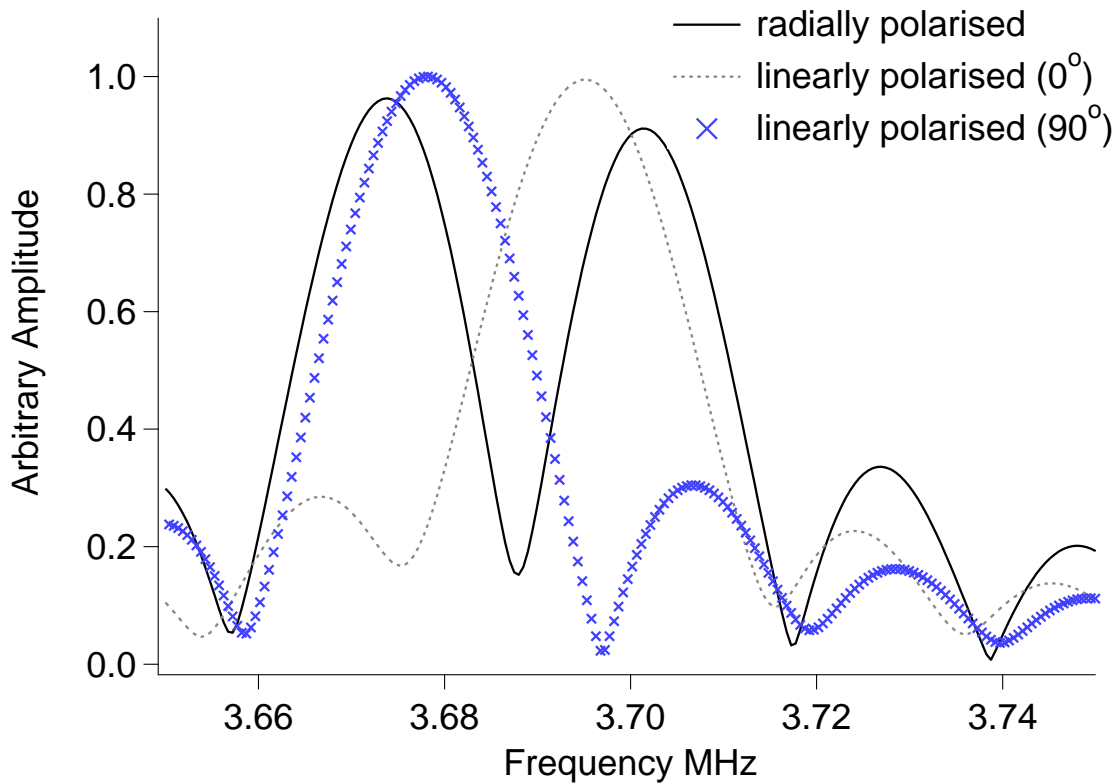


FIG. 1. Zoom in of peaks in the magnitude FFT spectrums without a Hanning function applied in the time domain data on a 2.99mm thick aluminium sample. The results from the radially polarized is shown as solid line and the results a linearly polarized EMAT orientated at 0° and 90° to the rolling direction, are shown as a dashed line and crosses respectively.

In the time domain, one can simply add the ultrasonic waveforms for the shear waves polarized at 0° and 90° to the rolling direction, to yield the same waveform that would be obtained using either a radially polarized EMAT or a linear polarized EMAT, polarized at 45° to the rolling direction. Having said this though, there will be some slight differences in the time domain waveforms due to the difference in the force distributions, but on producing the FFT, there would be insignificant difference between the magnitude transforms of the radially polarized time domain waveform and the sum of the two orthogonally polarized waveforms. It is sometimes naively thought that one can repeat this approach using the FFT magnitude transforms, adding the magnitude transforms from each of the orthogonal polarizations to yield the same result as the FFT magnitude transform that one obtains from the radially polarized shear wave data. The result of summing the two magnitude transforms, of a linearly polarized EMAT orientated at 0° and 90° to the rolling direction is shown as the solid line curve in figure 2, which is clearly totally different to the solid line plot of figure 1. This will be completely expected by anyone familiar with the use and theory of Fourier Transforms and is explained in more detail later on.

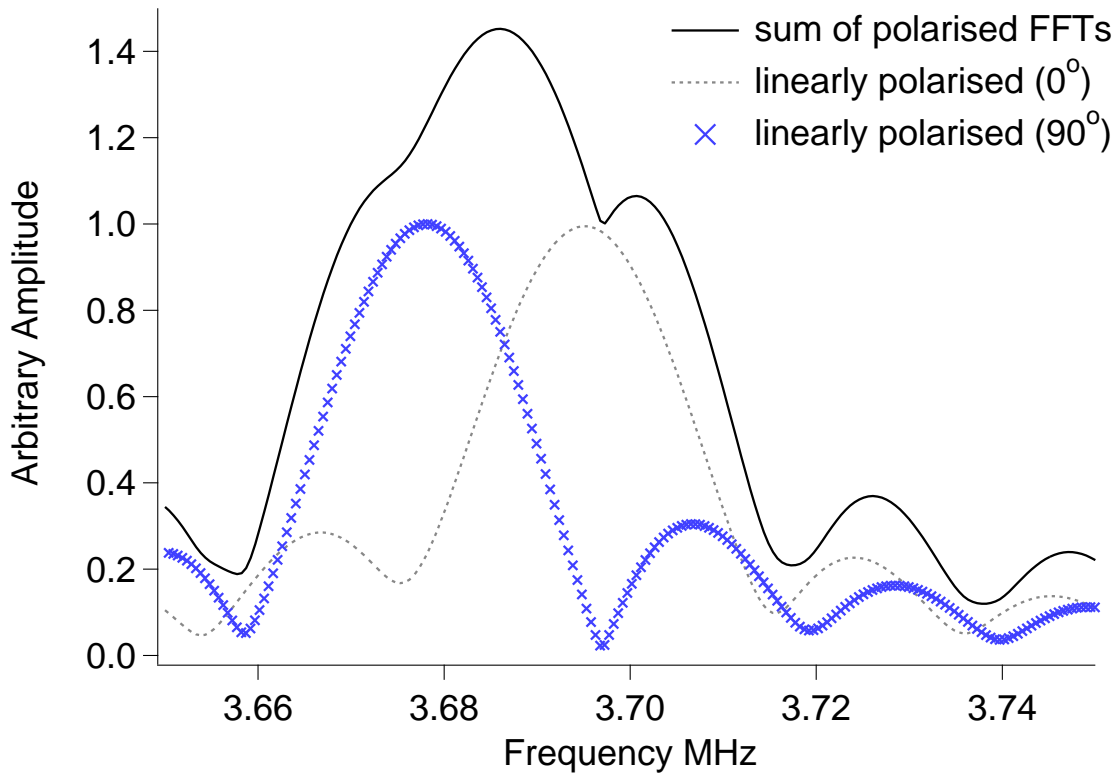


FIG. 2 Zoom in of peaks in the magnitude FFT spectrums without a Hanning function applied in the time domain data on a 2.99mm thick aluminium sample. The results from linearly polarized EMAT orientated at 0° and 90° to the rolling direction, are shown as a dashed line and crosses respectively, whilst the solid line is the linear addition of these two FFTs. This shows clearly, that the linear sum of the FFTs is completely different from the radially polarized EMAT seen in Fig. 1.

The peak in the FFT corresponds to the resonant frequency of the shear wave mode and thus in turn to the ultrasonic velocity of that mode, which is calculated by measuring the thickness of the sheet. One can immediately see the discrepancy between the peak positions between the linearly polarized waveforms and the radially polarized waveform. This arises from the Fourier Transform process itself and is explained in more detail later on. If one uses the position of the peaks of the three FFTs of figure 1 to calculate the shear wave velocities for the two polarizations, then one can attempt to calculate the ODCs. Calculating the ODCs using the radially polarized EMAT data (without Hanning) and linearly polarized peaks results in a 2% difference for the calculated W_{400} coefficient

and 39% difference for the calculated W_{420} , two-fold symmetry coefficients. The error in calculated velocity is only approximately 0.1% however, which means that there is no issue for using the data in thickness gauging applications. The source of these large differences in the calculated ODCs is due to the fact that the squared velocity difference must be used in the calculation. Previously we have shown that the peak shifting effect of birefringence can be reproduced reliably using simulations, whereby the two orthogonal polarizations can be modelled as sine waves or a waveform or periodic pulses [14]. This clearly demonstrates that the peak shifting or “bending” effect is due to the FFT, or more generally the Fourier Transform process.

II. BACKGROUND THEORY

It is the purpose of this section is to relate amplitude measurements to values of the resonant frequencies and this is done by introducing Fourier Transforms. Whilst the signal processing of real data is performed using FFT algorithms on a computer, we shall explain the source of the difference in peak positions of figure 1 using Fourier Transform integrals.

We define the complete Fourier Transform (CFT) by:

$$\hat{f}(\omega) = \int_0^L e^{-i\omega t} f(t) dt \quad (1)$$

In the case of our ultrasonic data, L would represent the temporal width of the window that contained the data. In the real data, the ultrasonic reverberations attenuate, so one could consider the waveform to be a convolution of a periodic function that generates ultrasonic pulses, with an exponential decay term. In what

follows, we neglect the exponential decay as it is not necessary to explain the nature of the difference in peak positions shown in figure 1, unless the rate of decay is particularly large, which in this case it is not.

For the simplified case that we consider here, the most general form of a signal with two distinct frequencies can be written as

$$f(t) = A_1 \cos(\omega_1 t + \gamma_1) + A_2 \cos(\omega_2 t + \gamma_2) \quad (2)$$

In which case, using simple integration

$$\hat{f}'(\omega) = A_1 [g(\omega, \omega_1) + g(\omega, -\omega_1)] \cos \gamma_1 + A_2 [g(\omega, \omega_2) + g(\omega, -\omega_2)] \cos \gamma_2 \quad (3)$$

where

$$g(\omega, \omega_n) = \frac{\sin[(\omega - \omega_n)L]}{(\omega - \omega_n)} \quad (4)$$

One can re-write equation 3 as

$$\hat{f}'(\omega) = A_1 [g'(\omega, \omega_1, \gamma_1) + g'(\omega, -\omega_1, \gamma_1)] + A_2 [g'(\omega, \omega_2, \gamma_2) + g'(\omega, -\omega_2, \gamma_2)] \quad (5)$$

Where g' is complex function and can be written as $g' = g'_R + i g'_I$, such that

$$g'_R(\omega, \omega_n, \gamma_n) = \frac{\sin\left[(\omega - \omega_n)\frac{L}{2}\right]}{(\omega - \omega_n)} \cos\left[(\omega - \omega_n)\frac{L}{2} - \gamma_n\right] \quad (6)$$

and

$$g'_I(\omega, \omega_n, \gamma_n) = \frac{\sin\left[(\omega - \omega_n)\frac{L}{2}\right]}{(\omega - \omega_n)} \sin\left[(\omega - \omega_n)\frac{L}{2} - \gamma_n\right] \quad (7)$$

It is the magnitude FFT that is of interest in this case and so one should consider the magnitude of the expression in equation 5, which takes the form

$$\left| \hat{f}'(\omega) \right| = \sqrt{\left\{ \begin{aligned} &A_1 \left[g_R(\omega, \omega_1, \gamma_1) + g_R(\omega, -\omega_1, -\gamma_1) \right] \\ &+ A_2 \left[g_R(\omega, \omega_2, \gamma_2) + g_R(\omega, -\omega_2, -\gamma_2) \right] \end{aligned} \right\}^2 + \left\{ \begin{aligned} &A_1 \left[g_I(\omega, \omega_1, \gamma_1) + g_I(\omega, -\omega_1, -\gamma_1) \right] \\ &+ A_2 \left[g_I(\omega, \omega_2, \gamma_2) + g_I(\omega, -\omega_2, -\gamma_2) \right] \end{aligned} \right\}^2} \quad (8)$$

Examining the equation above shows that there are cross terms between the two waves of frequencies ω_1 and ω_2 , and that the magnitude term consists of mixed terms, involving all the variables, A_1 and ω_1 , and A_2 and ω_2 .

III. EXPERIMENTAL RESULTS

By using a wave fitting procedure, it is possible to fit the analytical model developed in the previous section, to the experimental data obtained from a radially polarized EMAT, as seen in the following figures. The degree of fit was affected by the range of approximate starting values required, so often the best fit was obtained by trial and error until the difference between fit and experimental data was near optimum. The fitted coefficients were then used to calculate the respective velocity and texture coefficients. This demonstrates that the model of equation 8, reasonably describes and explains the source of the peak shifting effects, can be made to extract the true frequencies of the two orthogonal shear wave modes.

Figure 3 shows the magnitude FFT of the radially polarized shear wave data obtained on a 0.2mm thick aluminium sheet (alloy AL101332), together with an experimental fit to the data using equation 8. The 'fit' generated using equation 8, closely follows the experimental data, but there are small differences between the two, which is to be expected as the experimental waveform is generated by a wideband pulse rather than being a sine wave source, and the experimental data can also potentially contain other wavemodes that arise due to mode conversion [12]. In this case, the plate is so thin, that only one resonant mode pair can be observed at around 7.95 MHz. The next harmonic would be around 16 MHz, which is beyond the bandwidth of this particular EMAT system.

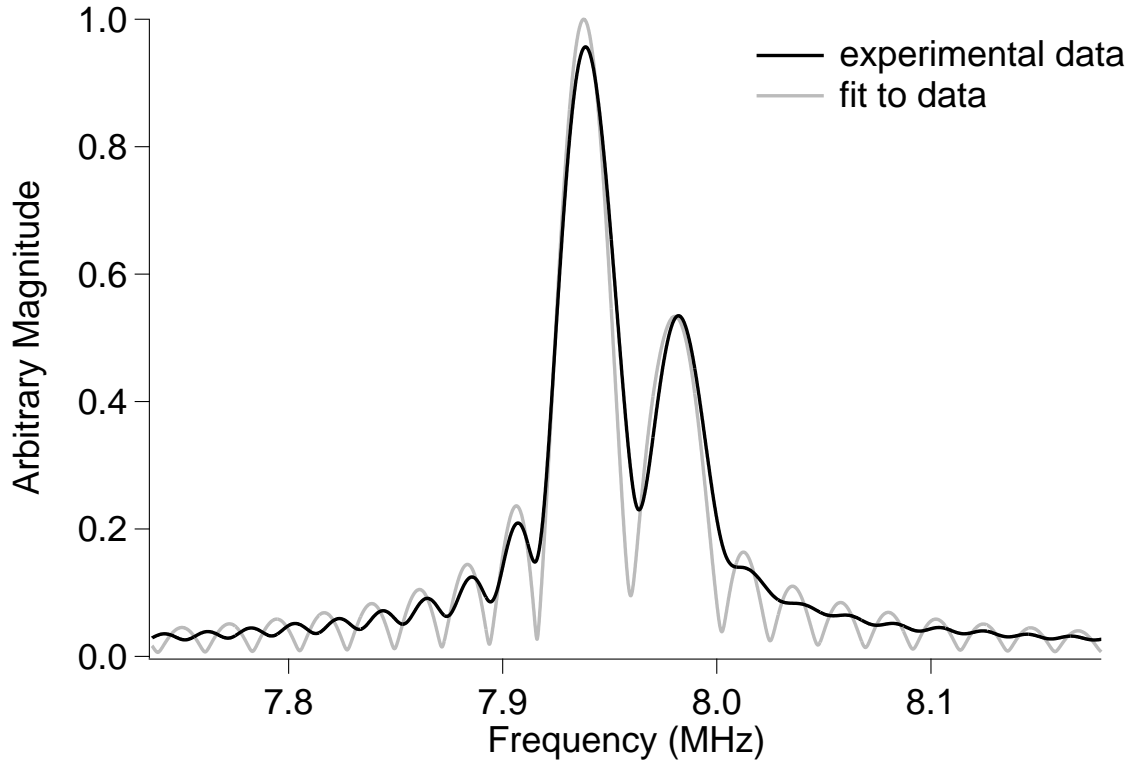


FIG. 3. Zoom in of harmonic peaks on the magnitude FFT from a 0.2mm (AL101332) thick aluminium sample using a radially polarized EMAT (black) compared against the complete model, equation 8, (grey) using best fit coefficients.

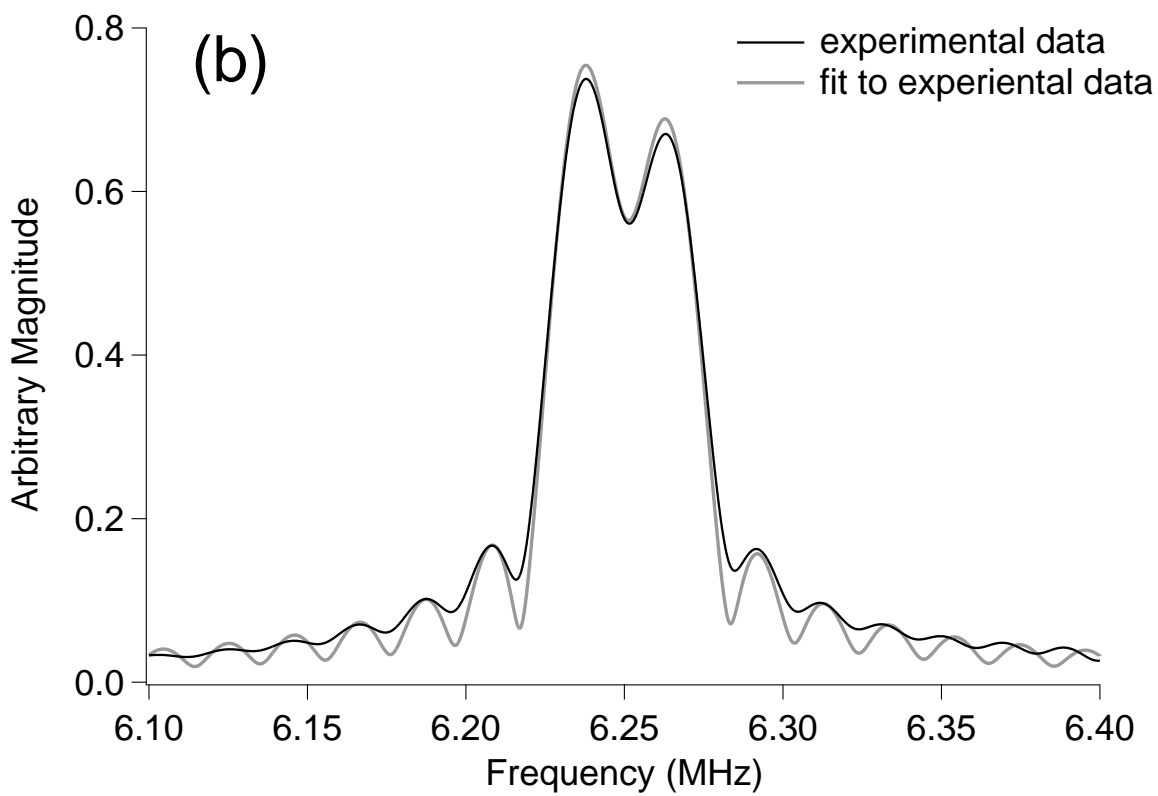
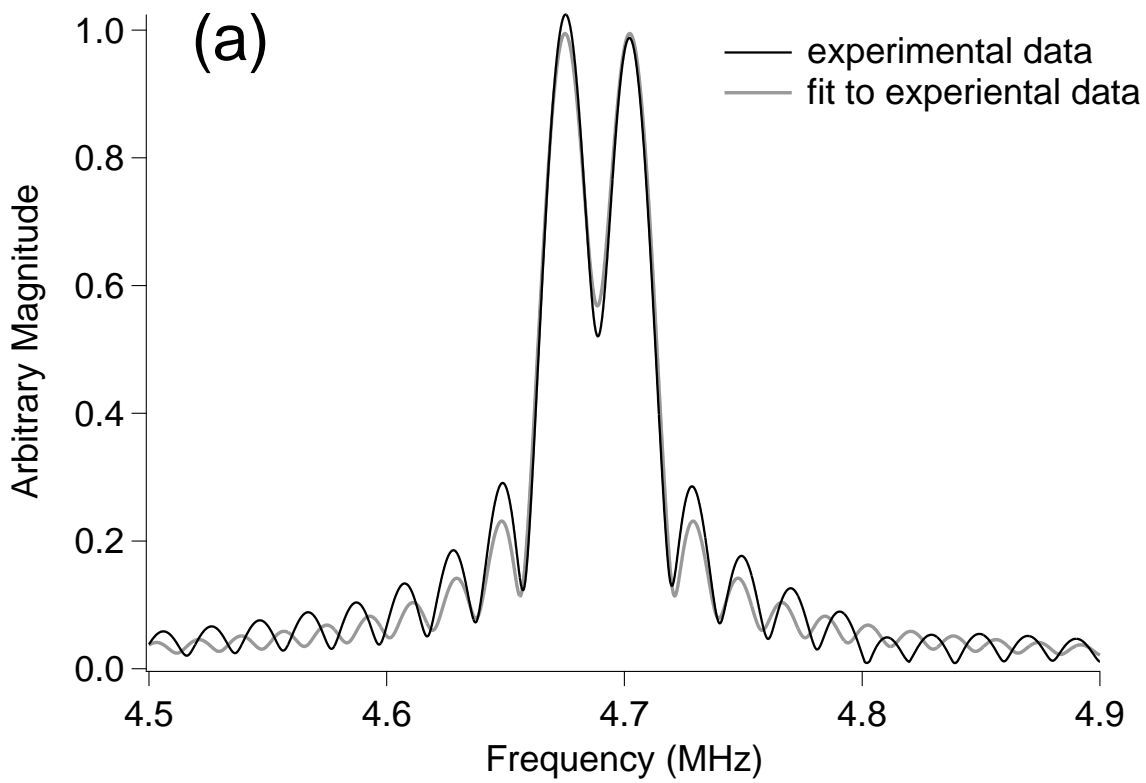
The ODCs are calculated from the FFTs. The peak maxima positions at each harmonic for the two linearly polarized shear wave FFT magnitude data are used to calculate the shear wave velocities for polarizations orientated at 0° and 90° to the rolling direction. The process is repeated for the radially polarized shear wave FFT magnitude data, on the understanding that these peak positions are liable to give incorrect values for the true reverberation frequencies. The values of the two reverberation frequencies obtained by fitting equation 8 to the radially polarized data are used to calculate the ultrasonic velocities polarizations orientated at 0° and 90° to the rolling direction. The calculated ODCs are shown in table 1. The table also shows the difference between the ODCs calculated from the different sources, and that calculated from the two magnitude FFTs of the shear wave data for polarizations orientated at 0° and 90° to the rolling direction.

Note that we expect the ODCs calculated from the two linearly polarized waveforms to yield the correct, or most accurate values of shear wave reverberation frequency or velocity and hence the most reliable value for the ODCs.

Table I. The ODCs, W_{400} and W_{420} , calculated for a 0.2mm (AL101332) thick aluminium sample using ultrasonic velocities determined from different methods.

	W_{400}	% diff. (W_{400})	W_{420}	% diff. (W_{420})
From two linearly polarized waveforms	2.075×10^{-2}	0	-1.136×10^{-2}	0
From curve fitting parameters	2.127×10^{-2}	2.5	-1.261×10^{-2}	11.0
From one radially polarized waveform	2.149×10^{-2}	3.6	-1.382×10^{-2}	21.6

Repeating the process for a thicker aluminium sample, allows us to observe more resonant modes than is observed for the 0.2 mm thick sheet [12]. In this case, using a 1mm thick sample, it is possible to record measurements of the first six or seven resonant modes, from which we have obtained peak maxima in the magnitude FFTs, or fitting parameters to the three largest amplitude peaks. These peaks occur at approximate frequencies of 4.7 MHz, 6.25 MHz and 7.8 MHz. The magnitude FFT of the radially polarized shear wave data, obtained on a 1.0 mm thick aluminium sheet (alloy AL101332), together with an experimental fit to the data using equation 8 are shown in figures 4a, 4b and 4c for these three peaks. The fit is performed three times to each of these peaks in turn by fitting around the approximate central frequency, over a range of 0.6 MHz. For example, the fit to the strongest peak shown in figure 4 was performed over the range 4.4 MHz to 5.0 MHz, and so on for the higher frequency peaks.



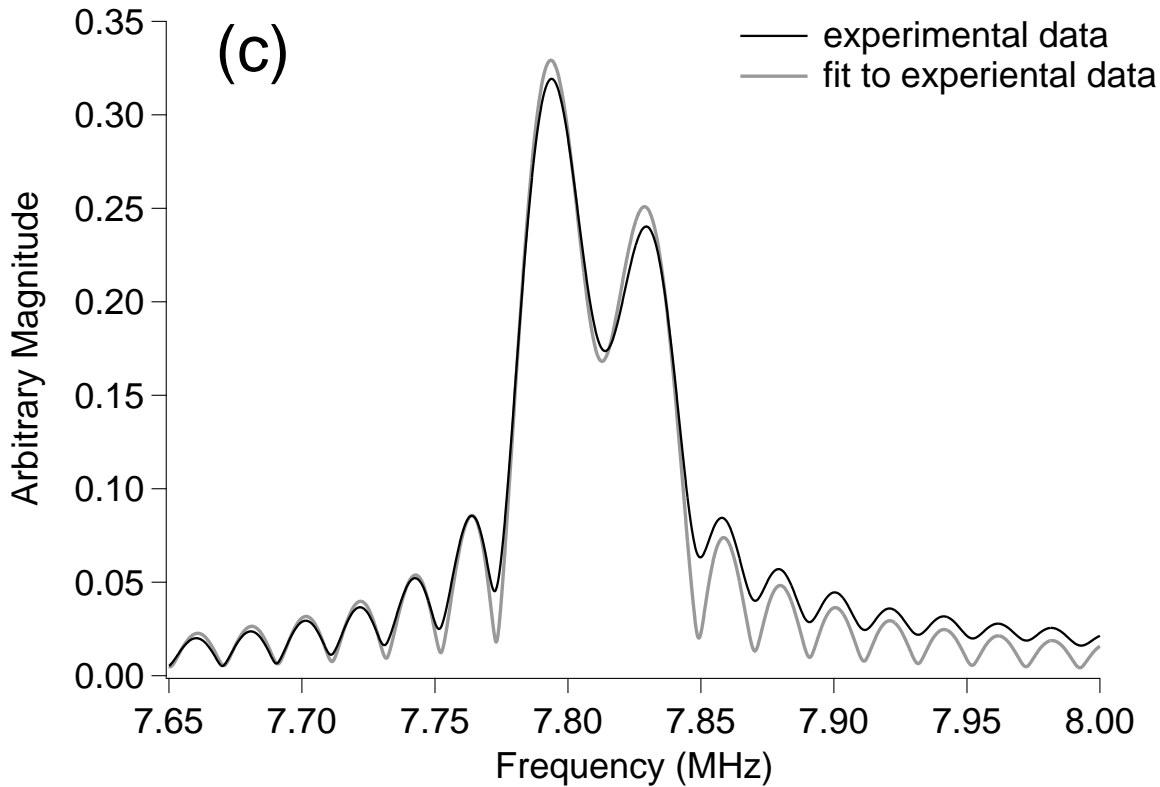


FIG. 4. Zoom in of different harmonic peaks on the same average magnitude FFT from a 1.0mm (AL104332) thick aluminium sample using a radially polarized EMAT (black line) compared against the complete model, equation 8, (grey line) using best fit coefficients.

Once again, it is clear that equation 8 provides a very plausible fit to the FFT of the experimental data. When one calculates the ODCs however, it is clear that significant discrepancies remain between the peak positions recorded directly from the linear polarized EMAT magnitude FFTs and from the radially polarized FFTs.

Moreover, it is clear that there appears to be a significant difference in the ODCs obtained from the linearly polarized shear wave measurements, using the maximum peak amplitude position for peaks (a), (b) and (c).

Given that this data comes from one waveform at the same location, on the same sample, it is clear that there is some discrepancy in calculating the ODCs from the different magnitude peaks in one FFT.

There are therefore two issues that one needs to deal with, the first being whether the time domain data from a linearly polarized broadband EMAT can be used to reliably determine the ODCs. The data presented below in table 2, indicates that one must exercise caution when using the FFT data obtained from a linearly polarized EMAT to determine the ultrasonic shear wave velocity, as the calculation of velocity based on the peak position of the FFT can produce variation in the answer of up to 0.5%. It has been shown in previous work though, that for practical thickness gauging purposes, if one normalises to one particular peak in the FFT and uses peak position to determine thickness, then very accurate values for changes in thickness can be measured [12].

Table II. Relative differences in the through thickness shear wave velocity calculated for a 1.0mm (AL104332) thick aluminium sample. For each polarization, peak positions of the first four SH shear wave modes on the magnitude FFT were measured, the velocity was calculated and then compared to the value obtained from the first peak position in the FFT.

	% difference polarized 0° to the rolling direction	% difference polarized 90° to the rolling direction
1 st peak	0	0
peak a	0.24	0.38
peak b	0.08	0.57
peak c	0.14	0.55

Putting the variability in the peak position in the FFT to one side, one can consider each peak of the magnitude FFT, radially polarized EMAT data in turn. The results from the second, third and fourth peaks in the FFT, as before are labelled as peaks a,b and c respectively. The fits to the data, shown in figures 4a, 4b and 4c yield the following values for the ODCs, shown in table 3. In table 3, the ODCs W_{400} and W_{420} are calculated for the two linearly polarized measurements, and the relative difference between the ODCs calculated from the radially polarized shear wave measurements are also considered. The ODCs calculated

by fitting the model of equation 8 to the radially polarized shear wave magnitude FFT data is clearly closer that obtained for the linearly polarized shear wave data, than the ODCs that are calculated from using the peak positions in the radially polarized shear wave magnitude FFT directly.

Table III. W_{400} & W_{420} calculated for a 1.0mm (AL104332) thick aluminium sample using the magnitude FFT data from linearly and radially polarized through thickness SH shear wave measurements.

peak (a)	W_{400}	% diff. (W_{400})	W_{420}	% diff. (W_{420})
From two linearly polarized waveforms	6.962×10^{-3}	0	-1.185×10^{-3}	0
From curve fitting parameters	6.954×10^{-3}	0.1	-1.273×10^{-3}	7.5
From one radially polarized waveform	6.955×10^{-3}	0.1	-1.398×10^{-3}	18.0

peak (b)	W_{400}	% diff. (W_{400})	W_{420}	% diff. (W_{420})
From two linearly polarized waveforms	6.758×10^{-3}	0	-0.986×10^{-3}	0
From curve fitting parameters	6.801×10^{-3}	0.6	-0.990×10^{-3}	0.4
From one radially polarized waveform	6.826×10^{-3}	1.0	-0.974×10^{-3}	1.2

peak (c)	W_{400}	% diff. (W_{400})	W_{420}	% diff. (W_{420})
From two linearly polarized waveforms	6.478×10^{-3}	0	-0.910×10^{-3}	0
From curve fitting parameters	6.587×10^{-3}	1.7	-0.979×10^{-3}	7.5
From one radially polarized waveform	6.686×10^{-3}	3.2	-1.110×10^{-3}	22.0

IV. CONCLUSIONS AND DISCUSSIONS

Previous work has shown that the observed peak shifting or “bending” in the through thickness shear wave magnitude FFT data that contains both polarizations simultaneously, could be reproduced using simulated time domain waveforms [14]. Here we have explained the source of the inconsistency between velocities calculated for the rolling and transverse directions using the peak positions in the magnitude FFT data from radially polarized EMATs and linearly polarized EMATs. It is due to interference between the individual frequencies present and arises as a result of applying the FFT to a finite set of time domain data. Modelling the two polarizations of shear wave waveforms as sine waves, allows us to use equation 8 to produce a theoretical fit to the experimental data. A good fit was achieved, as can be seen in figures 3,4a,4b and 4c. The degree of fit was affected by the range of approximate starting values provided, so often the best fit was obtained by trial and error until the difference between fit and experimental data was minimised. In some cases however it proved difficult to achieve an optimum fit, particularly if the maxima were not symmetric or displayed additional features such as mode converted signals, which was reflected in the degree of fit to data from a linearly polarized EMAT. Using the fit values supplied by the complete model, as opposed to the experimental peak positions provided a significant improvement in accuracy, as seen in tables 1 and 3.

The real ultrasonic waveforms are obviously not sinusoidal waves. We have made no attempt to account for ultrasonic beam diffraction, mode conversion, dispersion or attenuation in the model used. The aim of this work was to explain and demonstrate the source of the difference in peak position measurements from the magnitude FFTs of radially and linearly polarized shear wave data, which has been successfully done. This work shows that the interference of the peaks in the FFT for acoustically birefringent samples can be explained and demonstrated mathematically.

Analysis of the individual linearly polarized shear wave magnitude FFT data has shown that in general, the through thickness shear wave method has limited accuracy for determining the ODCs of the sample. It also demonstrates that care must be taken when using a similar method to determine the thickness of a sample using an assumed “known” shear wave velocity for the sample.

REFERENCES

- ¹G.A. Alers, Rev. Prog. Quant. Nondestr. Eval. **18**, 1695 (1999).
- ²R.J. Roe, J. Appl. Phys **36**, 2024 (1965).
- ³M.J.P. Musgrave, Math. and Phys Sci **40**, 131 (1985).
- ⁴M.J.P. Musgrave, Crystal Acoustics (Holden-Day 1970).
- ⁵M.L. Boas, Mathematical Methods In The Physical Sciences (John Wiley & Sons 1983).
- ⁶E Schneider, Optics and Lasers in Engineering **22**, pp. 305-323 (1995).
- ⁷A.V. Clark, Ultrasonics **23**, 21, (1985).
- ⁸Y. Pao, W. Sachse and H. Fukuoka, Physical Acoustics – Volume XVII (Academic Press 1984).
- ⁹CM Sayers, J. Phys. D **15**, 2157 (1982).
- ¹⁰H.M. Frost, Physical Acoustics – Volume XIV (Academic Press 1979).
- ¹¹E.R. Dobbs, Physical Acoustics – Volume X (Academic Press 1973).
- ¹²S. Dixon S, C. Edwards and S.B. Palmer, Ultrasonics **39**, 445 (2001).
- ¹³S. Dixon S, B. Lanyon and G. Rowlands, J. Phys. D: Appl. Phys. **39**, 506 (2006).
- ¹⁴M.P. Fletcher and S. Dixon, Rev. Prog. Quant. Nondestr. Eval. **26B**, 1244 (2007).